Electric control of dielectric droplets and films

D. A. Medvedev and A. L. Kupershtokh

View Online   Export Citation   CrossMark

Electric control of dielectric droplets and films

View Online   Export Citation   CrossMark

D. A. Medvedev[a)] (iD) and A. L. Kupershtokh (iD)

AFFILIATIONS

Lavrentyev Institute of Hydrodynamics SB RAS, 630090 Novosibirsk, Russia

Note: This paper is part of the Special Issue on the Lattice Boltzmann Method.
[a)]Author to whom correspondence should be addressed: dmedv@hydro.nsc.ru

ABSTRACT

We investigate the behavior of dielectric droplets and films placed onto a solid surface under the action of electric field of different configurations. The mesoscopic thermal multiphase lattice Boltzmann model [A. Kupershtokh, D. Medvedev, and I. Gribanov, "Thermal lattice Boltzmann method for multiphase flows," Phys. Rev. E **98**, 023308 (2018)] is used for simulation. Different configurations of electric field were produced by using dissected flat electrodes of various shapes. On a simple flat electrode, droplets elongate after the application of electric voltage. Quite different behavior was observed when the central round part of the electrode was made non-conductive. In this case, the droplet spreads under the action of a non-uniform electric field, and the breakup and the formation of an annular structure were observed. A film of dielectric liquid flowing along a solid surface made of conductive and non-conductive transversal stripes exhibits a variety of regimes. When the voltage is low, the action of electric field produces waves at the surface of liquid. At a high voltage, the liquid is pinned to the edges of stripes, and the flow may be stopped completely. The purpose of this article is precisely to attract experimenters to the study of this type of phenomena.

Published under an exclusive license by AIP Publishing. https://doi.org/10.1063/5.0074016

I. INTRODUCTION

Electric fields can be used for manipulating and controlling droplets and films of conducting and dielectric liquids. It is known that the free surface of liquid films subjected to a perpendicular strong electric field can be unstable with the formation of conic cusps.[2–6] Multiple conic cusps on the surface of liquid metal have been registered in an earlier work.[7] The first investigation of cone formation on the surface of water drops was carried out by Taylor.[3] The effect of DC electric fields on dielectric liquids is of great interest in many applications, including droplet and film manipulation, coating and surface drying, and cooling processes. In Refs. 3 and 8–14, the behavior of liquid sessile droplets on a solid surface under the action of gravity and electric field was studied. The phenomena of droplet deformation and motion in an electric field were also simulated. The equilibrium shape of a droplet lying on a solid surface (both dielectric and conductive) depends on the surface tension, as well as on the electrical and gravitational forces. It was shown also in Ref. 14 that sessile droplets can move along the hydrophobic surface in the direction of higher electric field strength. Both these effects provide for promising applications in droplet microfluidic technology.

The main non-dimensional numbers that determine the behavior of a droplet are the Bond number $\text{Bo} = \frac{gR^2\rho}{\sigma}$ and the electric Bond number $\text{Bo}_E = \frac{(\varepsilon_l-1)E^2R}{\sigma}$. Here, R is the droplet radius, g is the

acceleration due to gravity, σ is the surface tension, ε_l is the dielectric permittivity of the liquid phase, and $E = V/h$ is the average magnitude of the electric field between electrodes.

It is well known that the electric field not only changes the shape of the droplet but also can lead to unlimited lengthening of the droplet up to its destruction.[3,8] Above a certain critical value of Bo_E, the droplets cannot acquire a stable shape. This process of elongation and destruction of dielectric droplets was numerically simulated in Ref. 15. It was shown that the impulse character of the applied voltage played an important role due to transient process in elongation of droplets. The growth of droplet apex at the last stage is a phenomenon very similar to the explosive growth of perturbations on an initially flat free surface of dielectric films described in Ref. 6. The transversal electric field may generate instabilities in a film flow[16] and significantly influence the characteristics of film boiling.[17]

The lattice Boltzmann method (LBM) was first applied to simulate electrohydrodynamic flows in Refs. 18 and 19. This method allows one to take into account the surface tension on the liquid–vapor interface, the interaction of fluid with a solid substrate, as well as the external forces (electrostatic and gravitational).

In this work, we carry out three-dimensional modeling of dielectric drops and thin films in an electric field. For this purpose, the lattice Boltzmann method is used taking into account the action of

gravitational, capillary, and electrostatic forces. To control the behavior of dielectric droplets and thin films, certain configurations of non-uniform DC electric field are created using the dissected flat electrodes of various shapes. The equations for the electric field potential and for fluid dynamics are solved together.

II. LATTICE BOLTZMANN METHOD

A. LBM basics

The lattice Boltzmann method was first proposed in 1988.[20] It is based on the kinetic equation with a discrete set of velocities and a regular spatial lattice. The lattice vectors $\mathbf{e}_k$ and the velocity vectors $\mathbf{c}_k$ are related as $\mathbf{e}_k = \mathbf{c}_k \Delta t$ where Δt is the time step. The model with nine velocities (D2Q9) is commonly used in the 2D case, and the model with 19 velocities (D3Q19) is frequently applied in the 3D case. The evolution equation consists of the free streaming (propagation) of one-particle distribution functions f_k, the collisions, and the action of body forces as follows:

$$f_k(\mathbf{x}, t + \Delta t) = f_k(\mathbf{x} - \mathbf{e}_k, t) + \Omega_k\{f_k\} + \Delta f_k. \tag{1}$$

The collision operator Ω_k usually takes the form of the relaxation to local equilibrium values f_k^{eq} with a single relaxation time (Bhatnagar–Gross–Krook model[21])

$$\Omega_k = (f_k^{eq} - f_k)/\tau,$$

where τ is the non-dimensional relaxation time, or multiple relaxation times (MRT model[22,23]).

Equilibrium distribution functions depend on the local fluid density $\rho = \sum_k f_k$ and velocity $\mathbf{u} = \sum_k f_k \mathbf{c}_k / \rho$. They are usually chosen in the form of truncated Maxwellians as follows:[24]

$$f_k^{eq} = \omega_k \rho \left(1 + \frac{\mathbf{c}_k \cdot \mathbf{u}}{\theta} + \frac{(\mathbf{c}_k \cdot \mathbf{u})^2}{2\theta^2} - \frac{u^2}{2\theta}\right). \tag{2}$$

Here, ω_k are the weights for different lattice directions. In the D3Q19 model used in this work, they are equal to 1/3, 1/18, and 1/36 for the lattice vectors with lengths 0, h, and $\sqrt{2}h$, correspondingly. Here, h is the lattice spacing. The kinetic temperature θ is equal to $\theta = h^2/(3\Delta t^2)$ in the D2Q9 and D3Q19 models.

The last term in Eq. (1) represents the action of body force on the fluid. One of the popular choices for this term, the exact difference method (EDM)[25,26] expresses this term as a difference between equilibrium distribution functions before and after the action of the force as follows:

$$\Delta f_k = f_k^{eq}(\rho, \mathbf{u} + \Delta\mathbf{u}) - f_k^{eq}(\rho, \mathbf{u}), \quad \text{where} \quad \Delta\mathbf{u} = \mathbf{F}\Delta t/\rho. \tag{3}$$

The physical fluid velocity in this case is equal to[27]

$$\mathbf{u}^* = \mathbf{u} + \frac{\Delta\mathbf{u}}{2}.$$

B. Multiphase LBM

Two main approaches are used to simulate fluid flows with possible phase transitions between liquid and vapor. The pseudopotential model was first proposed in Ref. 28 and later further developed in Refs. 29 and 30. The free energy-based model was introduced in Refs. 31 and 32. In this work, we use the pseudopotential approach. In this case, the mesoscopic force is introduced, which acts between neighbor nodes as follows:

$$\mathbf{F}_{ph}(\mathbf{x}) = \psi(\rho(\mathbf{x})) \sum_{\mathbf{x}'} G(\mathbf{x}, \mathbf{x}')\psi(\rho(\mathbf{x}'))(\mathbf{x} - \mathbf{x}'). \tag{4}$$

The Green's function $G(\mathbf{x}, \mathbf{x}')$ is usually non-zero for nearest and next-nearest neighbors, the values are chosen so as to ensure isotropy of the interaction. In the Ref. 33, this force was expressed as a gradient of the pseudopotential as follows:

$$\mathbf{F} = -\nabla U.$$

The pseudopotential U is related to the equation of state $P = P(\rho, T)$ as follows:[33–35]

$$U = P - \rho\theta. \tag{5}$$

Equation (1) is usually written in the non-dimensional form, where distances are scaled by h, and time is scaled by Δt. It is also natural to scale the pressure, density, and temperature by the critical values P_c, ρ_c, T_c. In this case, the non-dimensional pseudopotential given by (5) should be expressed as follows:

$$\tilde{U} = k\tilde{P} - \tilde{\rho}\tilde{\theta}.$$

The coefficient k matches physical and non-dimensional (lattice) units and it is equal to[30]

$$k = \frac{P_c}{\rho_c}\left(\frac{\Delta t}{h}\right)^2.$$

It was proposed in Ref. 30 to write the pseudopotential as $U = -\Phi^2$ and express the force given by (4) in the form

$$\mathbf{F} = 2\big(A\nabla(\Phi^2) + (1 - 2A)\Phi\nabla\Phi\big).$$

The value of free coefficient A can be adjusted in order to ensure best agreement between the simulated coexistence curve and the theoretical one. It depends on the equation of state used. For the van der Waals equation of state used in this work, the value is $A = -0.152$.

C. LBM for electrohydrodynamic flows

The Helmholtz force acting on a dielectric fluid with electric permittivity ε in electric field is equal to

$$\mathbf{F}_e = -\frac{E^2}{8\pi}\nabla\varepsilon + \frac{1}{8\pi}\nabla\left(E^2\rho\left(\frac{\partial\varepsilon}{\partial\rho}\right)_T\right). \tag{6}$$

The first term is the action of electric field on inhomogeneous dielectric fluid, the second one is the electrostriction force. The electric field is connected with the electric potential φ as follows:

$$\mathbf{E} = -\nabla\varphi.$$

The electric potential was calculated by solving the Poisson equation in a medium with varying electric permittivity and without space charge, i.e.,

$$\nabla \cdot (\varepsilon\nabla\varphi) = 0,$$

by the finite-difference method using the method of simple iterations.

III. DROPLETS IN ELECTRIC FIELD

The behavior of a dielectric droplet placed on an electrode surface under the action of gravity and electric field was simulated. The
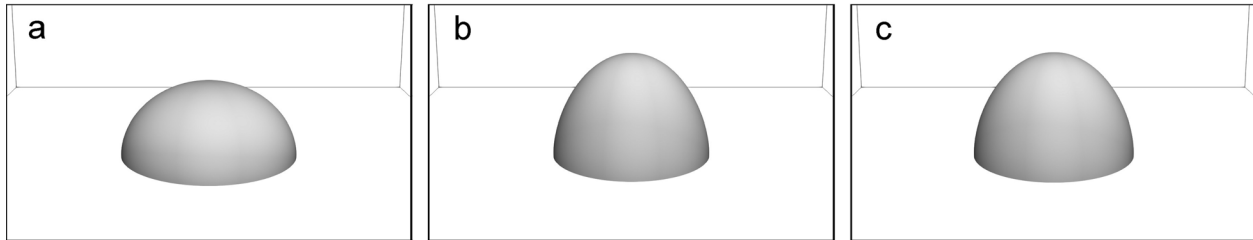
FIG. 1. Droplet elongation. Time (lattice units) $t = 0$ (a), 2000 (b), and 25 000 (c).

hydrodynamic boundary conditions were no-slip at the surface of electrodes and periodic at the sides of the computation area. The contact angle β was adjusted by introducing the force between fluid and solid surface. First, the values of the pseudopotential U [Eq. (5)] or, equivalently, of the function Φ were copied to the solid layer from the adjacent fluid layer. In this case, the contact angle is equal to $\beta = 90°$ (neutral wetting). Second, the following additional force between liquid and solid nodes was used:

$$\mathbf{F}_{fs} = B\rho(\mathbf{x}) \sum_k s(\mathbf{x} + \mathbf{e}_k)\mathbf{e}_k, \tag{7}$$

where $s = 0$ for fluid nodes and $s = 1$ for solid nodes. For $B > 0$, the fluid wets the surface ($\beta < 90°$) and for $B < 0$, the contact angle $\beta > 90°$. Another method to adjust the contact angle is to multiply the copied values of Φ by a coefficient C. The contact angle is $\beta < 90°$ for $C > 1$ and $\beta > 90°$ for $C < 1$. If $C \ll 1$, the surface becomes superhydrophobic.

Fixed potential was set at the conductive parts of the electrodes. At the non-conductive phases, the normal component of the electric field was set to zero as follows:

$$\frac{\partial \varphi}{\partial \mathbf{n}} = 0.$$

The density dependence of the electric permittivity was expressed in the Clausius–Mossotti form as follows:

$$\varepsilon = 1 + \frac{3\alpha\rho}{1 - \alpha\rho}. \tag{8}$$

The coefficient α was set to obtain the given electric permittivity ε_l of the liquid phase with an equilibrium density ρ_l.

The simulations were carried using the grid size $251 \times 251 \times 101$ lattice nodes. The static contact angle was $90°$ for all simulations.

Figure 1 shows the evolution of a droplet placed at an electrode in a relatively moderate electric field ($\mathrm{Bo}_E = 40$). After the application of voltage, the droplet elongates [Fig. 1(b)] and, after several oscillations, one obtains the final elongated shape.

The degree of deformation of the droplet is equal to

$$\Delta = \frac{h - r}{r} = 0.97.$$

Here, h is the droplet height and r is the radius of the base of the droplet.

When a droplet is placed at a superhydrophobic surface ($\beta \approx 180°$), its elongation in the transversal electric field is more prominent, and the droplet can jump under the action of the field.[11,13,36]

In the next series of simulations, the central round part of the lower electrode was made non-conductive (see Fig. 2). The radius of the insulating circle was 1.17 times larger than the initial droplet radius. In this case, the electric field is non-uniform: it is lower in the central part of the insulating circle and enhanced at its periphery. The liquid is pulled to the region of higher field, and the droplet spreads and acquires an oblate shape for the same field strength ($\mathrm{Bo}_E = 40$, Fig. 3).

The deformation in this case is $\Delta = -0.68$.

For a higher field magnitude ($\mathrm{Bo}_E = 80$), the pull is more pronounced. The droplet also spreads [Fig. 4(a)], but later it breaks in the center and finally acquires an annular shape [Fig. 4(b)]. Thus, the shape of droplets can be controlled by the electric field.

At the initial stage of spreading, instability of the dielectric boundary in the transversal electric field is observed, which produces protrusions visible at the contact line between the droplet and the electrode [Fig. 4(a)]. It is also interesting that the advancing contact angle is much lower than its equilibrium value of $90°$ due to the action of electric field.

When the droplet is placed not exactly at the center of the non-conductive part of the electrode (shifted by one lattice node to the right), it is pulled sideways and migrates outward from the non-conductive region (Fig. 5). The electric Bond number is in this case $\mathrm{Bo}_E = 20$.

A similar behavior of a bubble placed in a non-uniform electric field was observed in Ref. 37. The motion of a droplet in a non-uniform field produced by the point-plane electrode geometry was simulated in Ref. 14.

IV. LIQUID FILMS IN ELECTRIC FIELD

We simulated the evolution of a liquid film placed initially at the lower electrode under the action of gravity and electric field. The lower
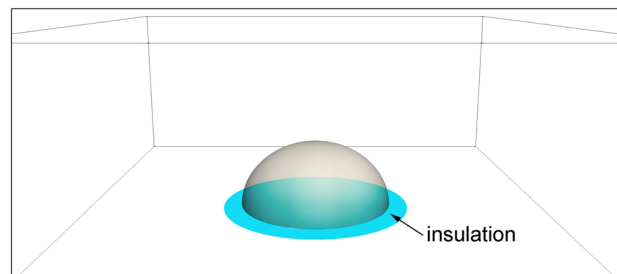

FIG. 2. Initial setup. Insulating region on electrode is shown with cyan.
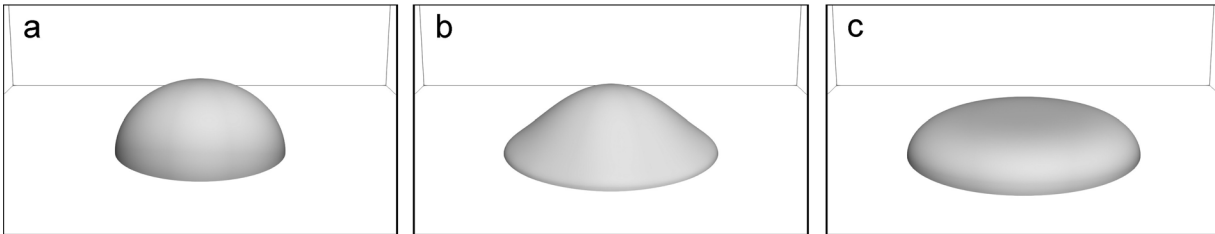
FIG. 3. Droplet spreading. Time (lattice units) $t = 0$ (a), 1000 (b), and 25 000 (c).
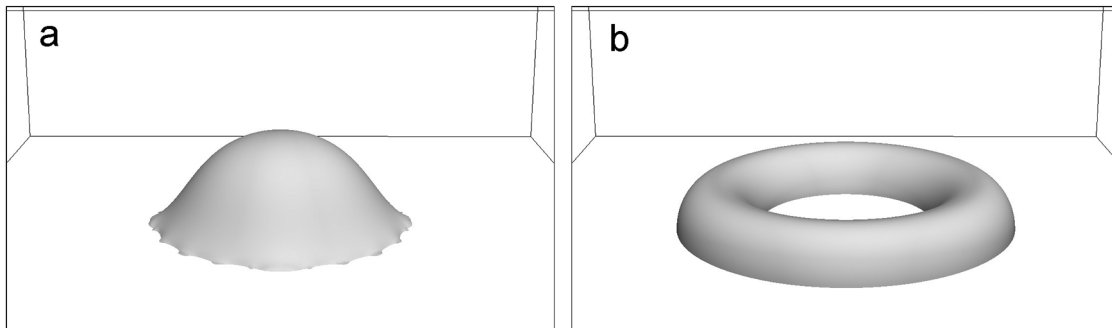

FIG. 4. Droplet spreading and breakup. Time (lattice units) $t = 300$ (a), and 6000 (b).
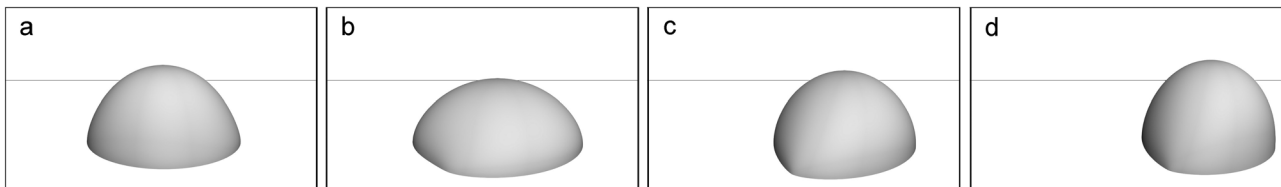

FIG. 5. Droplet migration. Time (lattice units) $t = 500$ (a), 3000 (b), 5500 (c), and 9000 (d).

electrode consisted of alternating conductive and non-conductive stripes of the same width placed perpendicular to the direction of the horizontal component of gravity. The initial height of the liquid layer was $h_0 = 20$ lattice units, the size of the calculation domain was $320 \times 320 \times 101$, the electric Bond number was $Bo_E = \frac{(\varepsilon_l - 1)E^2 h_0}{\sigma} = 160$.

On a slightly inclined surface (acceleration due to gravity in lattice units $g_z = 8 \times 10^{-5}$, $g_x = 10^{-5}$), the breakup of the film is observed (Fig. 6).

Banks of liquid are formed at the boundaries between the conductive and non-conductive parts of the lower electrode. These banks are pinned by the electric forces, and they are only slightly inclined to the right, in the direction of the horizontal component of gravity. Later, instability of the dielectric boundary in the transversal electric field develops [Fig. 6(d)], producing secondary bumps at each liquid bank.

When the inclination angle is higher (acceleration due to gravity $g_z = 8 \times 10^{-5}$, $g_x = 8 \times 10^{-5}$), the behavior of the film is completely different (Fig. 7). In this case, pinning does not occur, the action of electric forces produces waves at the surface of the flowing liquid.

Later, the waves may overturn, and surface instability also develops when the liquid surface comes closer to the upper electrode, which leads to increase in the electric field magnitude [Fig. 7(d)].

Figure 8 shows the evolution of the liquid film placed at the electrode with a ring-shaped non-conductive inset (inner radius of the ring $R_{in} = 50$, outer radius $R_{out} = 80$). The electric Bond number was $Bo_E = 80$, $g_z = 8 \times 10^{-5}$, $g_x = 0$, all other parameters were same as in the two previous cases.

After the application of voltage, the liquid is pulled outside of the non-conductive ring, producing a bump in the middle and a bank near the outer rim of the ring [Figs. 8(a) and 8(b)]. Then, the film breaks [Fig. 8(c)], and finally, a stable droplet is formed in the central part surrounded by a dry circle [Fig. 8(d)].

V. CONCLUSION

We investigated the behavior of dielectric droplets and films placed onto a solid surface under the action of electric fields of different configurations. The mesoscopic thermal multiphase lattice Boltzmann model[1] is used for simulation. A non-uniform field was
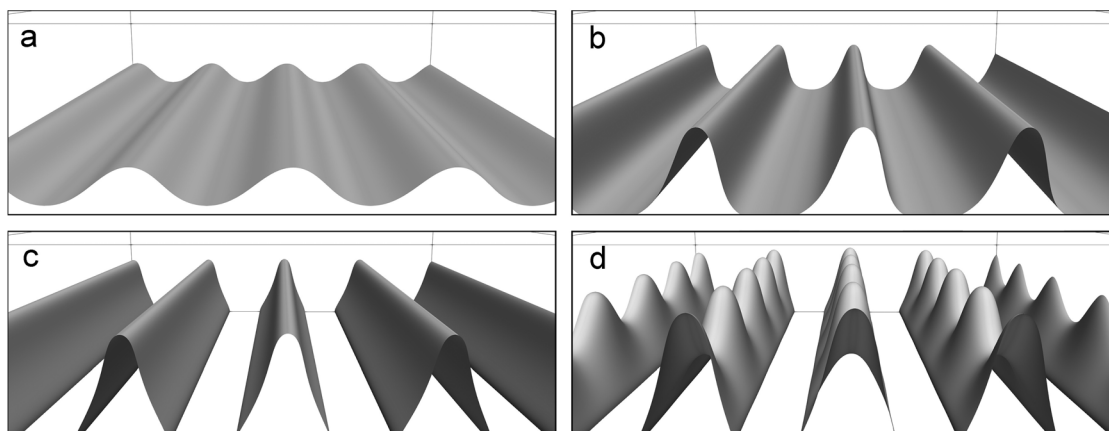
FIG. 6. Film breakup and pinning. Time $t = 500$ (a), 1000 (b), 2000 (c), and 20 000 (d).
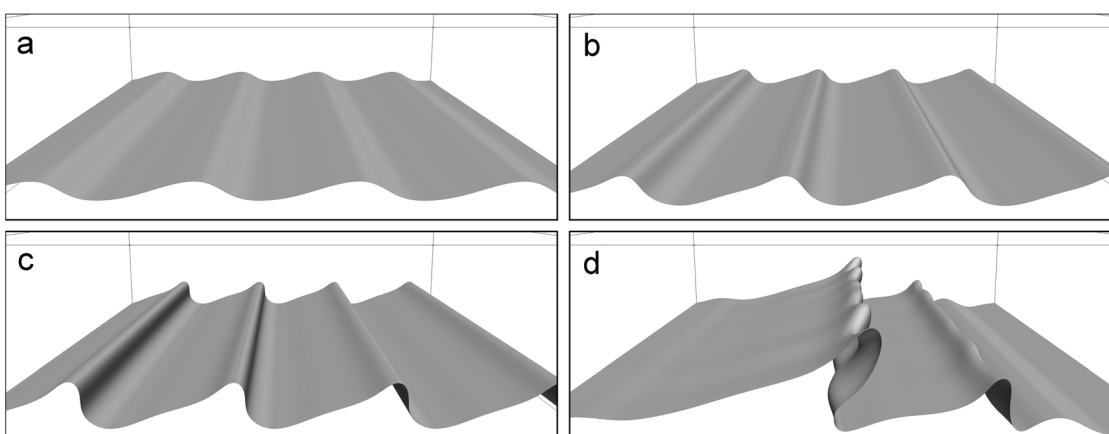

FIG. 7. Film flow and formation of waves. Time $t = 500$ (a), 1300 (b), 2000 (c), and 14 500 (d).
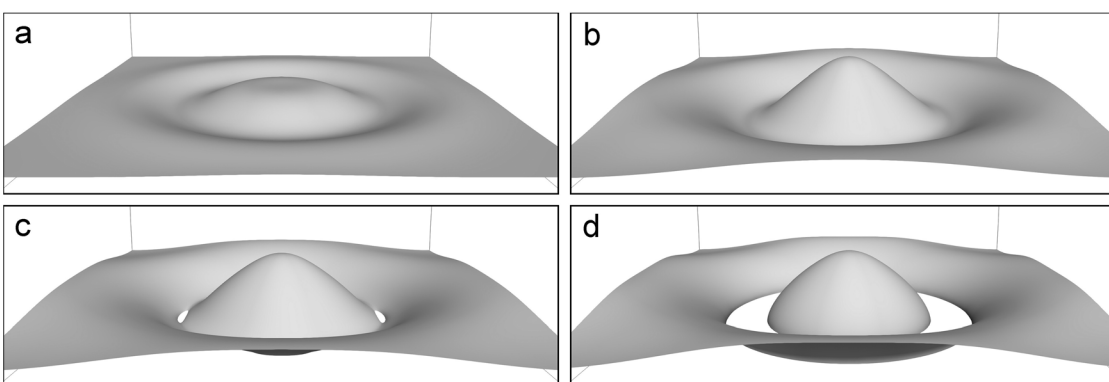

FIG. 8. Breakup of liquid film above the non-conductive ring. Time $t = 1000$ (a), 3000 (b), 6000 (c), and 9000 (d).

produced by inserting non-conductive parts of different shapes into the lower electrode. Without such inserts, droplets elongate after the application of electric voltage, the elongation increases with increasing voltage (and the corresponding electric Bond number).

In a non-uniform field, a qualitatively different behavior of droplets was observed. On electrodes with a non-conductive central part, the droplet spreads under the action of the non-uniform electric field. For a high enough electric Bond number, the breakup and the formation of an annular structure were observed.

A film of dielectric liquid flowing along a solid electrode made of conductive and non-conductive transversal stripes exhibits a variety of regimes depending on the relative strength of gravity and the electric field. When the voltage is low, gravity prevails and the action of electric field produces waves at the surface of the moving liquid. With a high voltage, the liquid is pinned to the edges of stripes, and the flow may be stopped completely. We also observed the breakup of liquid films and the formation of a dry area at the electrode with a ring-shaped non-conductive part.

Thus, the behavior of liquid droplets and films can be changed significantly by the application of electric field with different configurations. This may be used in order to control the liquid flow over a solid surface for different applications.

AUTHOR DECLARATIONS
Conflict of Interest

The authors have no conflicts to disclose.

DATA AVAILABILITY

The data that support the findings of this study are available from the corresponding author upon reasonable request.

REFERENCES

[1]A. Kupershtokh, D. Medvedev, and I. Gribanov, "Thermal lattice Boltzmann method for multiphase flows," Phys. Rev. E **98**, 023308 (2018).

[2]L. Tonks, "A theory of liquid surface rupture by a uniform electric field," Phys. Rev. **48**, 562–568 (1935).

[3]G. Taylor, "Disintegration of water drops in an electric field," Proc. R. Soc. A **280**, 383–397 (1964).

[4]N. Zubarev, "Formation of conic cusps at the surface of liquid metal in electric field," JETP Lett. **73**, 544–548 (2001).

[5]N. Zubarev, "Self-similar solutions for conic cusps formation at the surface of dielectric liquids in electric field," Phys. Rev. E **65**, 055301(R) (2002).

[6]K. Bobrov, N. Zubarev, and O. Zubareva, "Conditions for explosive growth of free surface perturbations for a dielectric liquid in a normal electric field in confined axisymmetric geometry," in *Proceedings of 20th IEEE International Conference on Dielectric Liquids* (IEEE, Roma, Italy, 2019), pp. 1–4.

[7]C. Zhou and S. Troian, "Multiplicity of inertial self-similar conical shapes in an electrified liquid metal," Phys. Rev. Appl. **15**, 044001 (2021).

[8]S. Reznik, A. Yarin, A. Theron, and E. Zussman, "Transient and steady shapes of droplets attached to a surface in a strong electric field," J. Fluid Mech. **516**, 349–377 (2004).

[9]L. Corson, C. Tsakonas, B. Duffy, N. Mottram, I. Sage, C. C. V. Brown, and S. Wilson, "Deformation of a nearly hemispherical conducting drop due to an electric field: Theory and experiment," Phys. Fluids **26**, 122106 (2014).

[10]D. Zong, Z. Yang, and Y. Duan, "Wettability of a nano-droplet in an electric field: A molecular dynamics study," Appl. Therm. Eng. **122**, 71–79 (2017).

[11]Y. Tian, H. Wang, Q. Deng, X. Zhu, R. Chen, Y. Ding, and Q. Liao, "Dynamic behaviors and charge characteristics of droplet in a vertical electric field before bouncing," Exp. Therm. Fluid Sci. **119**, 110213 (2020).

[12]M. Gibbons, A. Garivalis, S. O'Shaughnessy, P. Di Marco, and A. Robinson, "Evaporating hydrophilic and superhydrophobic droplets in electric fields," Int. J. Heat Mass Transfer **164**, 120539 (2021).

[13]K. Takeda, A. Nakajima, K. Hashimoto, and T. Watanabe, "Jump of water droplet from a super-hydrophobic film by vertical electric field," Surf. Sci. **519**, L589–L592 (2002).

[14]J. Liu and S. Liu, "Dynamics behaviors of droplet on hydrophobic surfaces driven by electric field," Micromachines **10**, 778 (2019).

[15]A. Kupershtokh, "Three-dimensional modeling of droplets dynamics of liquid dielectric on wettable surface in electric field," J. Phys. Conf. Ser. **1677**, 012067 (2020).

[16]A. Samanta, "Effect of electric field on an oscillatory film flow," Phys. Fluids **31**, 034109 (2019).

[17]V. Pandey, G. Biswas, and A. Dalal, "Effect of superheat and electric field on saturated film boiling," Phys. Fluids **28**, 052102 (2016).

[18]D. Medvedev and A. Kupershtokh, "Use of the lattice Boltzmann equation method to simulate charge transfer and electrohydrodynamic phenomena in dielectric liquids," in *Proceedings of the Second International Workshop on Electrical Conduction, Convection and Breakdown in Fluids, Grenoble, France*, edited by P. Atten and A. Denat (IEEE, 2000), pp. 60–63.

[19]A. Kupershtokh and D. Medvedev, "Lattice Boltzmann method in electrohydrodynamic problems," J. Electrost. **64**, 581–585 (2006).

[20]G. McNamara and G. Zanetti, "Use of the Boltzmann equation to simulate lattice-gas automata," Phys. Rev. Lett. **61**, 2332–2335 (1988).

[21]Y. Qian, D. d'Humières, and P. Lallemand, "Lattice BGK models for Navier–Stokes equation," Europhys. Lett. **17**, 479–484 (1992).

[22]P. Lallemand and L.-S. Luo, "Theory of the lattice Boltzmann method: Dispersion, dissipation Galilean invariance and stability," Phys. Rev. E **61**, 6546–6562 (2000).

[23]D. D'Humieres, I. Ginzburg, M. Krafczyk, P. Lallemand, and L.-S. Luo, "Multiple-relaxation-time lattice Boltzmann models in three dimensions," Philos. Trans. R. Soc. A **360**, 437–451 (2002).

[24]J. Koelman, "A simple lattice Boltzmann scheme for Navier–Stokes fluid flow," Europhys. Lett. **15**, 603–607 (1991).

[25]A. Kupershtokh, "New method of incorporating a body force term into the lattice Boltzmann equation," in *Proceedings of the 5th International EHD Workshop* (University of Poitiers, Poitiers, France, 2004), pp. 241–246.

[26]A. Kupershtokh, "Criterion of numerical instability of liquid state in LBE simulations," Comput. Math. Appl. **59**, 2236–2245 (2010).

[27]I. Ginzburg and P. Adler, "Boundary flow condition analysis for the three-dimensional lattice Boltzmann model," J. Phys. II **4**, 191–214 (1994).

[28]X. Shan and H. Chen, "Lattice Boltzmann model for simulating flows with multiple phases and components," Phys. Rev. E **47**, 1815–1819 (1993).

[29]R. Zhang and H. Chen, "Lattice Boltzmann method for simulations of liquid-vapor thermal flows," Phys. Rev. E **67**, 066711 (2003).

[30]A. Kupershtokh, D. Medvedev, and D. Karpov, "On equations of state in a lattice Boltzmann method," Comput. Math. Appl. **58**, 965–974 (2009).

[31]M. Swift, W. Osborn, and J. Yeomans, "Lattice Boltzmann simulation of non-ideal fluids," Phys. Rev. Lett. **75**, 830–833 (1995).

[32]M. Swift, E. Orlandini, W. Osborn, and J. M. Yeomans, "Lattice Botzmann simulations of liquid-gas and binary fluid systems," Phys. Rev. E **54**, 5041–5052 (1996).

[33]Y. Qian and S. Chen, "Finite size effects in lattice-BGK models," Int. J. Mod. Phys. C **8**, 763–771 (1997).

[34]X. He and G. Doolen, "Thermodynamic foundations of kinetic theory and lattice Boltzmann models for multiphase flows," J. Stat. Phys. **107**, 309–328 (2002).

[35]R. Nourgaliev, T. Dinh, T. Theofanous, and D. Joseph, "The lattice Boltzmann equation method: Theoretical interpretation, numerics and implications," Int J. Multiphase Flow **29**, 117–169 (2003).

[36]A. Kupershtokh and D. Medvedev, "Dielectric droplet on a superhydrophobic substrate in an electric field," in *Proceedings of 20th IEEE International Conference on Dielectric Liquids* (IEEE, Roma, Italy, 2019), pp. 1–4.

[37]A. Nemykina and D. Medvedev, "Behavior of a bubble in dielectric liquid in uniform and non-uniform electric fields," Interfacial Phenom. Heat Transfer **7**, 323–330 (2019).